OPEN ACCESS Freely available online

PLOS ONE

Stiffening-Induced High Pulsatility Flow Activates Endothelial Inflammation via a TLR2/NF-κB Pathway

Yan Tan[1,2¤a], Pi-Ou Tseng[1], Daren Wang[2], Hui Zhang[2¤b], Kendall Hunter[2], Jean Hertzberg[1], Kurt R. Stenmark[2], Wei Tan[1]*

1 Department of Mechanical Engineering, University of Colorado at Boulder, Boulder, Colorado, United States of America, **2** Department of Pediatrics, University of Colorado at Denver, Aurora, Colorado, United States of America

Abstract

Stiffening of large arteries is increasingly used as an independent predictor of risk and therapeutic outcome for small artery dysfunction in many diseases including pulmonary hypertension. The molecular mechanisms mediating downstream vascular cell responses to large artery stiffening remain unclear. We hypothesize that high pulsatility flow, induced by large artery stiffening, causes inflammatory responses in downstream pulmonary artery endothelial cells (PAECs) through toll-like receptor (TLR) pathways. To recapitulate the stiffening effect of large pulmonary arteries that occurs in pulmonary hypertension, ultrathin silicone tubes of variable mechanical stiffness were formulated and were placed in a flow circulatory system. These tubes modulated the simulated cardiac output into pulsatile flows with different pulsatility indices, 0.5 (normal) or 1.5 (high). PAECs placed downstream of the tubes were evaluated for their expression of proinflammatory molecules (ICAM-1, VCAM-1, E-selectin and MCP-1), TLR receptors and intracellular NF-κB following flow exposure. Results showed that compared to flow with normal pulsatility, high pulsatility flow induced proinflammatory responses in PAECs, enhanced TLR2 expression but not TLR4, and caused NF-κB activation. Pharmacologic (OxPAPC) and siRNA inhibition of TLR2 attenuated high pulsatility flow-induced pro-inflammatory responses and NF-κB activation in PAECs. We also observed that PAECs isolated from small pulmonary arteries of hypertensive animals exhibiting proximal vascular stiffening demonstrated a durable ex-vivo proinflammatory phenotype (increased TLR2, TLR4 and MCP-1 expression). Intralobar PAECs isolated from vessels of IPAH patients also showed increased TLR2. In conclusion, this study demonstrates for the first time that TLR2/NF-κB signaling mediates endothelial inflammation under high pulsatility flow caused by upstream stiffening, but the role of TLR4 in flow pulsatility-mediated endothelial mechanotransduction remains unclear.

Citation: Tan Y, Tseng P-O, Wang D, Zhang H, Hunter K, et al. (2014) Stiffening-Induced High Pulsatility Flow Activates Endothelial Inflammation via a TLR2/NF-κB Pathway. PLoS ONE 9(7): e102195. doi:10.1371/journal.pone.0102195

Editor: Joseph Najbauer, University of Pécs Medical School, Hungary

Received September 21, 2013; **Accepted** June 16, 2014; **Published** July 16, 2014

Funding: This study was funded in part by grants from the National Institutes of Health (NIH) (HL K25-097246 to W.T., HL-14985-36 to K.R.S.) and the American Heart Association (13GRNT16990019 to W.T.). The funders had no role in study design, data collection and analysis, decision to publish, or preparation of the manuscript.

Competing Interests: The authors have declared that no competing interests exist.

* Email: wei.tan-1@colorado.edu

¤a Current address: Department of Geriatrics, Nanfang Hospital, Guangdong, China
¤b Current address: Department of Pediatrics, Shengjing Hospital and China Medical University, Shenyang, China

Introduction

It is increasingly accepted that large artery stiffening, which commonly occurs with aging, hypertension, diabetes, etc., contributes to the microvascular abnormalities of the kidney, brain, and eyes that characterize these pathophysiologic conditions [1–5]. In pulmonary hypertension, a group of progressive and fatal diseases, it has also become evident that stiffening of large proximal pulmonary arteries occurs, often early, in the course of this spectrum of diseases that have been conventionally characterized by dysfunction and obliteration of small distal pulmonary arteries [6]. However, while both clinical and animal studies convincingly demonstrate an association between proximal artery stiffening and distal artery dysfunction, few studies have examined the underlying cellular and molecular mechanisms through which these pathologic features might be inherently linked.

Besides being a conduit between the heart and distal vasculature, elastic proximal arteries act as a cushion or hydraulic buffer transforming highly pulsatile flow into semi-steady flow through the arterioles [4]. Normally, the so-called arterial windkessel effect is efficiently performed such that the mean flow, which reflects the steady-state energy, is well maintained throughout the arterial tree, whereas flow pulsatility, which reflects the kinetic energy of flow, is reduced by the deformation of compliant proximal arteries [7,8]. Thus, flow pulsatility in distal arteries is usually low, due to kinetic energy dissipated by the proximal compliance. In the cases of aging and diabetes in the systemic circulation or various forms of pulmonary hypertension, stiff proximal arteries reduce their cushion function to modulate flow pulsation, extending high flow pulsatility into distal vessels where the pulse remnant might be reduced via smooth muscle contractility. Therefore, proximal stiffening may contribute to small artery abnormalities found in high flow, low impedance organs including the kidney, brain, eye, and lung [2,3,5]. It is thus clear that a better understanding of the contribution of pulsatility (the kinetic component) of unidirectional physiologic flow to molecular changes in the downstream vascular endothelium is

necessary for a better understanding of the effects of artery stiffening on cardiovascular health.

The endothelium, uniquely situated at the interface between the blood and the vessel wall, is an efficient biological flow sensor that converts flow stresses to biochemical signals, which in turn modulate vascular tone, infiltration of inflammatory cells and other cell activities important in vascular remodeling [9–11]. Endothelial cells (ECs) not only sense the mean magnitude of flow shear stress, but also discriminate among distinct flow patterns [10]. While a majority of studies on EC mechano-transduction of flow involve turbulent or disturbed flows with low wall shear stress ($\leq$2 dyne/cm^2) simulating atherosclerosis-related flow conditions [9–11], few systems exist to examine the impact of stiffening on EC physiology. We have previously established flow pulsatility, a stiffening-related flow parameter, as a determinant of pulmonary artery endothelial function [12]. In response to unidirectional high pulsatility flow (HPF) with the mean shear stress remaining at a physiological level (12 dyne/cm^2), ECs demonstrate pro-inflammatory and vasoconstrictive responses [12], though the mechanisms involved in the ECs' ability to sense and respond to pulse flow remained unclear. Growing evidence supports the role of TLRs, a family of integral membrane proteins, in the initiation and progression of vascular diseases that are associated with disturbed blood flow such as atherosclerosis. It was found that ECs are the first cells to display increased TLR expression in early lesions of atherosclerotic prone vessels [13]. It is also known that ECs normally express TLR4 and a very low level of TLR2, which is further reduced under physiological flow conditions [14]. The TLRs are essential factors not only in the innate immune response, functioning as the first line of defense against pathogens, but also in homeostasis mediating cell responses to stress and danger signals [13]. Upon activation, TLRs may activate several downstream signaling nuclear factors, thus leading to a local inflammatory response [15]. Though the key role that TLRs play in atherosclerosis is becoming recognized [16], few studies have examined possible roles of TLRs in other vascular diseases, particularly those absent of turbulent flow. We therefore sought to test the hypothesis that reduced upstream compliance in the large pulmonary arteries enhances high flow pulsatility in distal vessels which in turn induces endothelial inflammation via a TLR/NF-κB pathway. To address this hypothesis, we developed an *ex-vivo* model flow system to simulate the effects of stiffening of upstream arteries on the downstream endothelial function. In addition to the model system, we also determined whether TLR expression in small PAECs was increased with pulmonary hypertension in calves and humans whose large pulmonary arteries are characterized by significant stiffening [17,18].

Methods

Endothelial cell isolation and culture

Bovine PAECs were isolated from pulmonary arterial endothelium of normal (CO-ECs) and pulmonary hypertensive (PH-ECs) calves. The use of calves conforms to the Guide for the Care and Use of Laboratory Animals published by the United States National Institutes of Health, and was approved by the Institutional Animal Care Use Committee (IACUC) at the Colorado State University. Animals were euthanized using an overdose of pentobarbital as recommended by the Panel on Euthanasia of the American Veterinary Medical Association. The cell isolation of the endothelium from calf small arteries (after 4th generation) as intact monolayers, involved brief pretreatment with Dispase (Becton Dickinson Inc, Franklin Lakes, NJ) followed by a single scrape with a flexible plastic scraper. Cell monolayers were plated onto at least 10 culture dishes, either plastic or covered with 1% denatured type I collagen (gelatin) in complete D-Valine MEM medium (Sigma Inc, Saint Louis, MO) with 10% fetal bovine serum. Freshly separated cells were characterized for their expressions of MCP-1 and TLRs. Primary cultures were confirmed to be free of contamination with smooth muscle cells by thorough screening of at least 2 culture dishes using immunostaining for smooth muscle marker. For all the *in vitro* flow experiments, CO-ECs at passages 4–8 were used. There was little difference in TLR2 and TLR4 expression or their responsiveness to various stimuli between cells of different passages.

Preparation methods of silicone tubes as mechanical equivalents to pulmonary artery

To employ silicone tubes that simulate the buffering function of proximal elastic pulmonary arteries in normal and hypertensive conditions, we utilized silicone elastomers with various elastic moduli to form tubes, and placed them upstream to the flow chambers where PAECs were cultured (Figure 1A). Silicone elastomer base and curing agent (Sylgard184 elastomer kit, Dow Corning Inc, Midland, MI) were mixed at different ratios to obtain varied elastic moduli. To determine appropriate polymer compositions that simulate the compliance function of large pulmonary arteries, we studied how the ratio between the base solution and the crosslinker (curing agent) influences the elastic modulus of silicone elastomer. The tensile modulus of samples was measured with a tensile tester (Instron Inc, Norwood, MA). For this study, we used a base-to-crosslinker ratio of 36:1 for a "soft" tube and 10:1 for a "stiff" tube, which respectively simulate buffering function of normotensive and hypertensive proximal pulmonary arteries, while the thickness and length of both tubes were kept the same ($\sim$0.3 mm thick, 5 cm long). Fabrication of silicone tubes involves a repeated dip-cure process. Briefly, a stainless steel cannula (14 G) was briefly dipped into the silicone prepolymer mixture with a predetermined base-to-crosslinker ratio, and then placed into an oven set at 60°C for 4 h to cure the polymer coating on the cannula. This was followed by repeating the dipping process with the same silicone elastomer mixture and back to the oven for additional 4 h. The ultrathin silicone tube was then carefully removed from the stainless steel cannula. The resultant silicone tubes (cut into a length of 5 cm) exhibit appropriate distensibility and cushion function to mimic the flow buffering of normotensive and hypertensive pulmonary arteries, respectively.

Mechanical properties of silicone elastomers were characterized with tube compliance testing and stress-strain tensile testing. For tube compliance testing that reveals the pressure-diameter relationship, a tube was loaded onto a custom-made fixture through tube adapters, using suture threads to secure the tubes near the adapters on both ends. The tube was then connected to a flow network via pressure gauges (Living Systems Instrumentation, Burlington, VT) on both ends of the tube. The pressure in the tube was controlled using varying speed of a water pump, to obtain a steady pressure from 0 mmHg to 100 mmHg, with a gradual increment. At each pressure, images of the tube dilatation were taken using a Canon EOS 450D camera (Canon, Tokyo, Japan). These images were analyzed using a customized script in MatlabVR (MathWorks, Natick, MA) to obtain the tube diameter at each pressure point.

To measure the mechanical properties of human pulmonary arteries, we performed ultrasonic imaging to determine the pressure-diameter relationship *in vivo* and stress-strain tensile testing *in vitro* to measure the elastic moduli of pulmonary arteries in the circumferential direction. With informed consent and/or

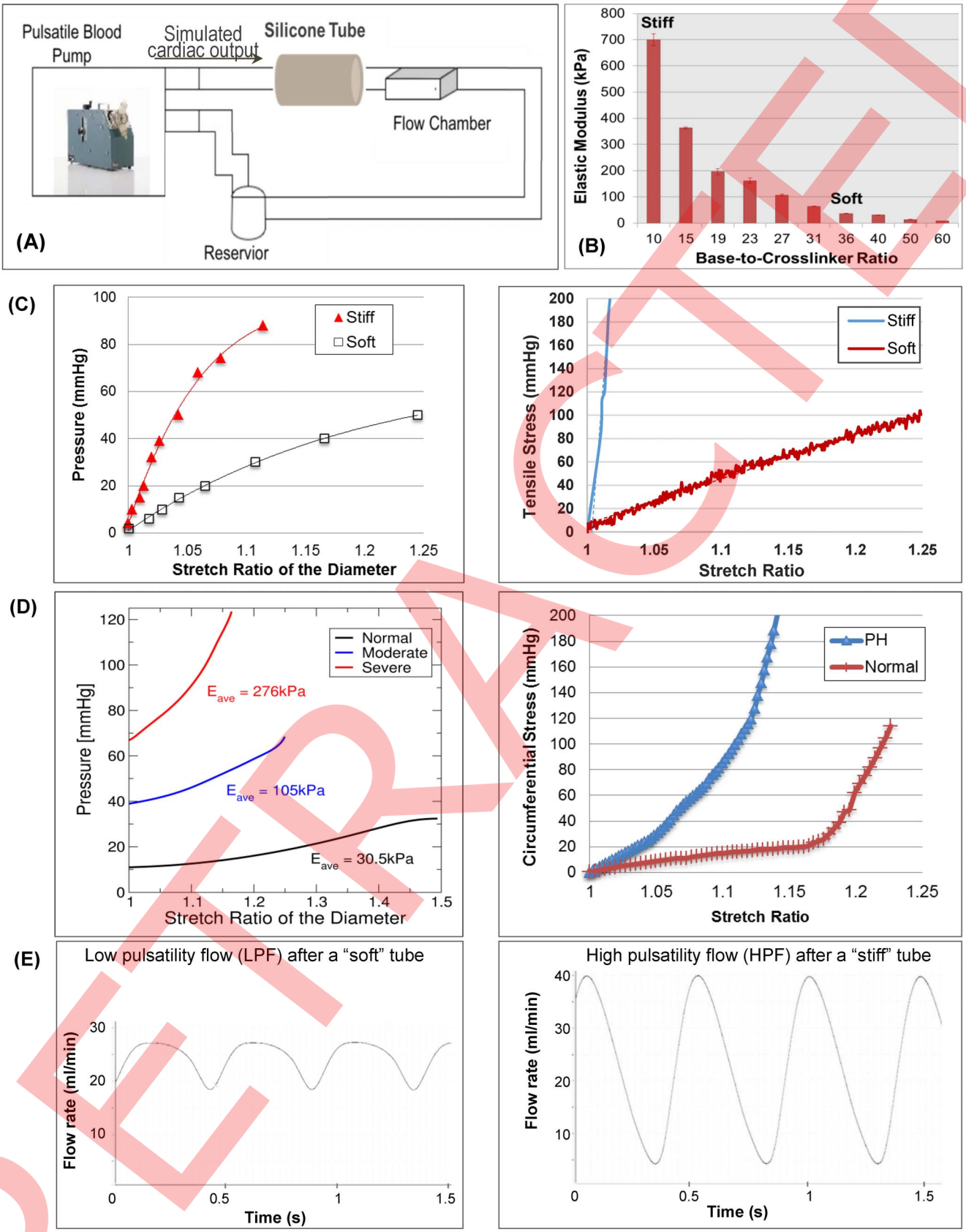

Figure 1. Experimental setup for flow studies. (A) Illustration of the flow circulation system. (B) Silicone tubes with various elastic moduli were prepared with varying the base-to-crosslinker ratio. (C) Pressure-diameter relationship curves of "soft" and "stiff" tubes showing their difference in compliance (left) and representative tensile stress-strain curves of "soft and "stiff" silicone materials (right). (D) Representative biomechanical

characterization curves of human pulmonary arteries from normal (control) patients or from those with moderate or severe pulmonary hypertension (PH) using *in vivo* measures (left) or *ex vivo* tensile stress-strain tests (right). (E) Representative pulsatile flow waveforms taken at the exit of "soft" and "stiff" tubes.
doi:10.1371/journal.pone.0102195.g001

assent when applicable, we studied 36 patients undergoing evaluation of reactivity using oxygen and/or nitric oxide in the cardiac catheterization laboratory at the Children's Hospital in Denver, CO. Pediatric patients ranged in age from 1 month to 19 years (mean = 6.5±5.2 yrs, 19 males). Written consent was obtained from the next of kin, caretakers, or guardians on the behalf of the minors/children participants involved in this study. All clinical studies had approval from the Colorado Multiple Institutional Review Board.

Pressure was obtained within the right pulmonary artery (RPA) using 5- or 6-fr Swan-Ganz catheters (Transpac IV, Abbott Critical Care Systems, Abbott Park, IL), while CMM-TDI was obtained of the RPA wall from the suprasternal short-axis view, which provides a long-axis representation of the RPA with the walls perpendicular to the ultrasound beam angle. Immediately prior to acquisition, the ultrasound beam was swept through the long axis of the RPAs to locate maximal diameter; acquisition then occurred along this beamline. For each patient, measurements were typically obtained at room air, considered the baseline, and toward the end of each clinical challenge.

Tensile testing of silicone elastomers and pulmonary arteries

Tensile testing was performed using an MTS Insight2 electromechanical testing system (MTS Systems Corp., Eden Prairie, MN, USA). For testing of silicone elastomers, all materials were cut to 5 mm wide by 25 mm long. Uniaxial tensile testing with a strain rate of 5 mm per min was performed on samples. All elastomers showed linear behavior, and a linear fit of the stress–strain curve was used to determine the modulus. For testing of main pulmonary arteries from human, stress-strain data was acquired with an MTS Insight2 system with a 5 N load cell. Tissue strip widths were measured with digital calipers. The circumferential strips were tested in an auxiliary environmental chamber with the same buffer solution as storage and pressure diameter testing. Tissues were prestrained by applying nine extension-relaxation cycles, and data was collected on the tenth cycle. Arteries cut in the circumferential direction were strained at a rate of 10% strain per second.

Experimental setup and protocol for flow studies on cells

The flow system used for examining PAECs under mimetic pulse flow conditions is demonstrated in Figure 1A. The circulating medium contained 7% Dextran (MP-products Inc, Solon, OH) and 1% penicillin/streptomycin, as its viscosity was close to blood viscosity. A pulsatile blood pump (Harvard Apparatus Inc; Holliston, MA) was used to circulate the medium, going through a silicone tube, a flow chamber with cell culture, a medium reservoir, and then back to the pump. Herein, the pump simulates the heart function generating cardiac output, while the silicone tube simulates the flow buffering or cushion function of proximal large arteries, and the flow chamber holds the endothelium to simulate the distal pulmonary vascular bed. Each component was connected by stiff polystyrene tubing. For flow measurements, a flow meter (Alicat Inc, Tucson, AZ) was placed before the flow chamber. Silicone tubes expanded during the systolic stage and contracted during the diastolic stage in response to the simulated cardiac output, behaving like large elastic arteries (Movie S1 and Movie S2). Tubes different in distensibility, "soft" and "stiff" tubes, were in use (Figure 1B). Through these tubes, we generated two different pulsatile flows for the cell experiments. Both pulsatile flows had the same mean flow rate with a mean flow shear stress of 14 dynes/cm^2 and run at the same frequency.

To examine the response of PAECs to flow conditions, plain microscope glass slides were chemically functionalized with 20% of aqueous sulfuric acid and then coated with 6% of 3-aminopropyl-triethoxysilane in acetone. After silanization, glass slides were treated with 1.5% of glutaraldehyde and then coated with 25 μg/ml fibronectin. Bovine PAECs at a concentration of 6.0×10^5 per ml were seeded on the fibronectin-coated slides that were transferred to the flow chamber apparatus after cells reached confluence. Then, PAECs were exposed to either high or low pulsatility flow for 24 h with 4 h preconditioning under steady flow. PAECs grown in the absence of flow (the static condition) were used as a control. After PAECs were exposed to different flows, they were collected and analyzed for gene expression of ICAM-1, VCAM-1, MCP-1, E-selectin, IKKα and IKKβ using real-time PCR and for protein expression of MCP-1, TLR2 and TLR4 using western blotting. Nuclear translocation of NF-κB was analyzed by immunofluorescence.

Pharmacological treatments on cells

To determine the role of TLR2 and/or NF-κB in the flow-induced inflammatory response, BPAECs were incubated for 2 h with TLR2/4 inhibitor OxPAPC (Invivogen, San Diego, CA, 30 μg/ml), TLR4 inhibitor CLI-095 (Invivogen, 1 μg/ml) and NF-κB inhibitor BAY11-7082 (Enzo Life Sciences Inc, Farmingdale, NY, 5 μmol/l), respectively. After pretreatment with drugs, cells were exposed to the pulsatile flow conditions, using the medium containing OxPAPC (30 μg/ml), CLI-095 (1 μg/ml) and BAY11-7082 (5 μmol/l), respectively.

Gene knockdown with siRNA

Short interfering (si) RNA targeting TLR-2 (5′-rGrArArUrUrArGrArCrArCrCrUrArGrGrUr ArArUrGrUrGGA-3′ and 5′-rUrCrCrArCrArUrUrArCrCrUrArGrGrUrGrUrCrUrArArUrUrCrUrG-3′) and TLR-4 (5′-rGrGrArGrCrArArGrArArCrUrArCrArGrArArUrUrUrGrCCA-3′ and 5′-rUrUrCrCrUrCrGrUrUrCrUrUrGrArUrGrUrCrUrUrArArArCrGrGrU-3′) were obtained from IDT (Integrated DNA Technologies, Coralville, IA). Scrambled siRNA (5′- rCrCrArGrUrCrGrCrArArACrGrCrGrAr CrU -3′ and 5′- rArArCrArGrUrCrGrCrGrUrUrUrGrCrGrArC -3′) was used as a control. Cells were seeded for transfection at a density of 6.0×10^5 per ml on a fibronectin-coated slide and cultured for 16 h. Cells were transfected with siTLR2 at a concentration of 50 nmol/L, using DharmaFECT siRNA transfection reagents (Dharmacon Inc., Lafayette, CO) according to the manufacturer's instruction. Culture medium was changed after 8 h to remove the transfection reagent. Transfected cells (after 48 h) were used in flow experiments.

Real-time qPCR

Total cellular mRNA from each sample was extracted using RNeasy Mini Kit (Qiagen; Hilden, Germany) according to the manufacturer's instructions. Complementary DNA was synthesized from 1 μg of total cellular mRNA using iScript cDNA Synthesis Kit (Bio-Rad, Hercules, CA). Real-time quantitative PCR primers are designed using Primer 3 Software to target bovine species for genes related to pro-inflammatory adhesion

molecules including ICAM-1, VCAM-1 and E-selectin, chemokines such as MCP-1, and signaling molecules such as TLR2, TLR4, IKKα and IKKβ. The sequences of these genes are listed in Table 1. The SYBR Green I assay and the iCycler iQ real-time PCR detection system (Bio-Rad MyiQ; Hercules, CA) were used for quantitatively detecting real-time PCR products from 12 ng of reverse-transcribed cDNA. PCR thermal profile consisted of 94°C for 3 min, followed by 42 cycles of 94°C for 45 s, 50°C for 45 s and 77°C for 1 min. Genes were normalized to the housekeeping gene hypoxanthine-xanthine phosphoribosyl transferase (HPRT) and the fold change relative to static condition was determined using the ΔΔCT method.

Western blotting

Western blot analyses were performed as per the manufacturer's suggestions (Invitrogen, Carlsbad, CA). Antibodies used here include: rabbit polyclonal antibody against bovine MCP-1 (1:500 dilution; Kingfisher Biotech, St. Paul, MN), rabbit polyclonal antibody against TLR2 (1:100 dilution; Bioss Inc, Woburn MA), mouse monoclonal antibody against TLR4 (1:100 dilution; Acris Antibodies Inc, San Diego, CA) and mouse monoclonal antibody against GAPDH (1:20,000 dilution; Sigma Inc, Saint Louis, MO). The molecular sizes for MCP-1, TLR2, TLR4 and GAPDH are 8.8 kDa, 84 kDa, 96 kDa and 36 kDa, respectively.

Immunofluorescent staining

Cells were fixed in PBS-buffered 4% paraformaldehyde at room temperature, and then blocked with 3% BSA in PBS for 30 min. Subsequently, they were incubated with a primary antibody overnight at 4°C. NF-κB p105/p50 (specificity to p65, 1:500 dilution; Novus, Littleton, CO) were used. After washing with PBS, cells were incubated with a secondary antibody. Nuclei were counterstained with DAPI. Microscopic imaging was performed with a Zeiss fluorescent microscope and/or a Leica DMRXA microscope (Solms, Germany). Tissue cryosections were similarly stained with human TLR2 (1:50 dilution; Imgenex).

Data and statistical analysis

All data are expressed as mean ± SEM, and the number of sample studied (n) is ≥3. Using the power analysis with Graphpad StateMate, the power values of all data were found to be greater than 80%. One-Way ANOVA was used to determine effects of flow pulsatility on gene expression. If significant difference exists, Student's t-test for one-to-one comparison and Tukey for post-hoc analysis were used to compare means of each individual group. A P value <0.05 was considered significantly different.

Results

Development of the mimetic flow circulatory system

To determine the effects of upstream compliance and flow pulsatility on proinflammatory responses and underlying molecular signaling in downstream PAECs, we stimulated PAECs with pulsatile flows downstream to "soft" or "stiff" tubes which, by virtue of differences in tube deformation, dampened the pulsatile flow from the pump to various degrees (Figure 1). Silicone elastomers with various elastic moduli were constructed and then utilized to form tubes, and placed upstream to the flow chambers where PAECs were cultured (Figure 1A). As shown in Figure 1B, the elastic modulus of silicone tubes decreased with the increase of the base-to-crosslinker ratio. Two tube conditions were chosen as representatives to respectively simulate buffering function of normotensive and hypertensive proximal pulmonary arteries, as it was previously shown that the elastic modulus of large pulmonary arteries in normotensive subjects (calf or human) was in the range of 20–50 kPa, whereas that in hypertensive subjects could increase anywhere from 2–10 fold [17–21]. To illustrate the different cushion functions and mechanical properties of "stiff" and "soft" tubes, Figure 1C (left) shows tube distensibility with pressure-diameter relationship curves obtained with a series of static flow pressures and Figure 1C (right) illustrates their elasticity with representative stress-strain curves. Using ultrasonic imaging and tensile testing on artery strips obtained in the circumferential direction, we also showed representative pressure-diameter relationship and tensile stress-strain curves for human pulmonary arteries from different patient groups (Figure 1D). Though mechanical behaviors of pulmonary arteries are more complicated, the results showed that the tubes could serve as good mechanical equivalents to upstream arteries. Earlier studies on the relationship between arterial compliance and arterial elastic modulus showed that the thickness of the arterial wall plays an important role in determining the arterial compliance in addition to elastic modulus. Though hypertensive arteries exhibited both tissue thickening and progressive matrix remodeling such as increased collagen content which increases arterial elastic modulus, we simplified the tube preparation by making tube thickness constant while using the tube distensibility and flow buffering function as the mimetic criteria. Figure 1E demonstrates cushion function of the tubes by showing varied pulsatile flows at the exit of the tubes which modulate the input flow waveform of simulated

Table 1. Bovine primer sequences for real-time RT-PCR.

	FWD	REV
MCP-1:	CGCCTGCTGCTATACATTCA	ACACTTGCTGCTGGTGACTC
VCAM-1:	GAGCTTGGACGTGACCTTCT	TGGGTGGAGAATCATCATCA
ICAM-1:	GACTTCTTCAGCTCCCCAAG	CCCACATGCTATTTGTCCTG
E-Selectin:	CTCCCCGTCCAAGAACTACA	CGCCTCTACCTGTCCTTGAG
TLR 2:	TTCTGAATGCCACAGGGCGG	TGCAGCCACGCCCACATCAT
TLR 4:	ATGCCAGGATGATGGCGCGT	ACCTGTACGCAAGGGTCCCA
IKKa:	CCGGAATTCGAGCGGCCCCCGGGGCTG	AAACTCGAGTTATTCTGTTAACCAACTCCAATC
IKKβ:	CCGGAATTCAGCTGGTCACCTTCCCTGCC	AAAGTCGACTTACGAGGCCCGCTCCAGGCT
HPRT:	CTGGCTCGAGATGTGATGAA	CAACAGGTCGGCAAAGAACT

doi:10.1371/journal.pone.0102195.t001

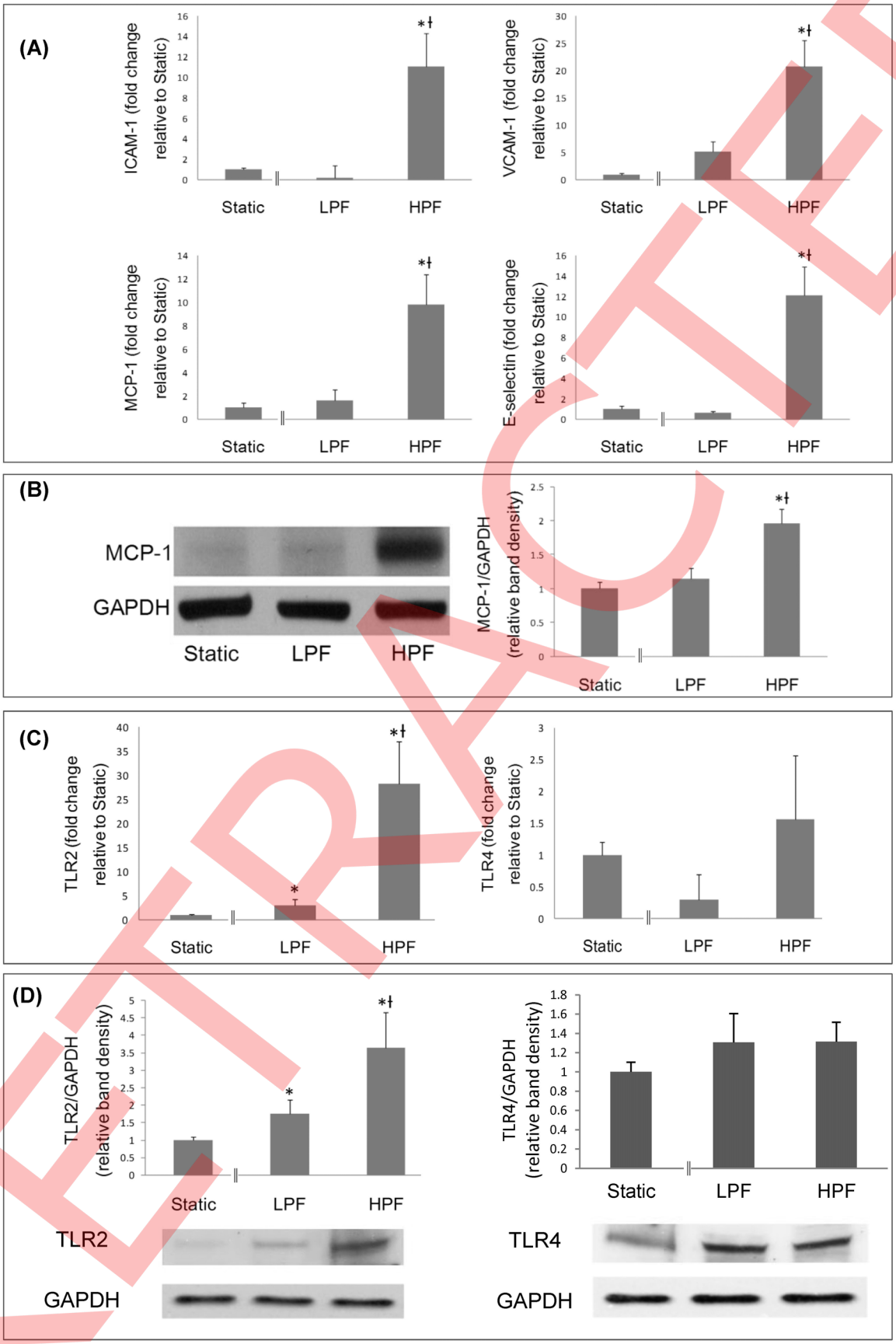
(A)
ICAM-1 (fold change relative to Static)
VCAM-1 (fold change relative to Static)
MCP-1 (fold change relative to Static)
E-selectin (fold change relative to Static)
Static
LPF
HPF
*†
(B)
MCP-1
GAPDH
MCP-1/GAPDH (relative band density)
(C)
TLR2 (fold change relative to Static)
TLR4 (fold change relative to Static)
(D)
TLR2/GAPDH (relative band density)
TLR4/GAPDH (relative band density)
TLR2
TLR4

Figure 2. Proximal stiffening induces proinflammatory response and upregulates TLR2 expression in downstream bovine PAECs. (A-B) High pulsatility flow (HPF), due to the use of a "stiff" tube upstream to cell culture, upregulated proinflammatory molecule mRNA (ICAM-1, VCAM-1, MCP-1 and E-selectin) and protein (MCP-1) in healthy PAECs, compared to low pulsatility flow (LPF) or to static conditions. (C-D) The mRNA and protein expression of TLR2 but not TLR4 in PAECs was highly upregulated by HPF. *: $p<0.05$ versus Static, †: $p<0.05$ versus LPF.
doi:10.1371/journal.pone.0102195.g002

cardiac output. Both pulsatile flows had the same mean flow rate with a mean flow shear stress of 14 dynes/cm^2 and run at the same frequency. Figure 1E shows the flow pulsatility indices after the "stiff" and "soft" silicone tubes are 1.5 and 0.5, respectively. The pulsatility levels *in vivo* fall within a close range of pulsatility levels used here. Previous studies showed that the mean flow pulsatility in the large PAs ranged from 4.4 to 5.1 *in vivo*, while the flow pulsatility in the pulmonary capillaries decreased to ~1 [22,23]. When there is no elastic deformation on the wall, a pulsatility value greater than 1 could exert detrimental effects on the endothelium.[24]

Proximal stiffening increases flow pulsatility and augments inflammatory responses in downstream PAECs

As shown in Figure 2A, endothelial cells exposed to HPF (with a pulsatility index of 1.5 for 24 h), induced by increased stiffness of the proximal silicone tube, exhibited markedly higher levels of ICAM-1, VCAM-1, E-selectin and MCP-1 expression than cells exposed to low pulsatility flow (LPF). Changes in gene expression were confirmed at the protein level by western blot analyses for MCP-1 (Figure 2B). Limitations on the availability of bovine-specific antibodies prevented evaluation of protein expression of other gene products ICAM-1, VCAM-1 and E-selectin. No significant changes in the expression of these genes were found between cells exposed to LPF (with a pulsatility index of 0.5) generated by "soft" tube, when compared to those maintained under the static condition (Figure 2A).

HPF upregulates TLR2 expression but not TLR4 expression in PAEC

To explore whether HPF alters TLR expression, PAECs exposed to LPF or HPF were analyzed for TLR2/4 expression using real-time PCR and western blot analysis, after 24 h of flow stimulation. Figures 2C-D show that both gene and protein expression of TLR2 was significantly upregulated in the cells exposed to HPF, compared to those exposed to static or LPF conditions. No statistically significant changes in TLR4 protein levels were observed in cells stimulated by different flow conditions. Hereafter, LPF condition was used as control for HPF in order to illuminate the differences in flow conditions related to upstream artery stiffness in the normal vs hypertensive subjects.

Inhibition or knockdown of TLR2 results in suppression of HPF-induced endothelial inflammation

To determine whether TLR2- or TLR4- mediated signaling contributed to the inflammatory responses induced by HPF, the TLR4 inhibitor CLI-095 and the TLR2/TLR4 inhibitor OxPAPC (a TLR2 specific pharmacological inhibitor is not available) were used. As shown in Figures 3A-B, PAECs treated with OxPAPC (inhibiting both TLR2 and TLR4) but not CLI-095 dramatically reduced proinflammatory adhesion molecule (ICAM-1, VCAM-1, E-selectin) and cytokine (MCP-1) gene expression in response to HPF. To further validate the role of TLR2 signaling in mediating the effects of HPF, we performed studies using ECs pretreated with TLR2 siRNA. Knockdown of TLR2 expression was confirmed with real-time PCR by showing decreased TLR2 expression in the cells treated with TLR2 siRNA compared to those treated with scrambled siRNA (data not shown). siRNA knockdown of TLR2 resulted in significant downregulation of inflammatory gene expression in PAECs exposed to HPF (Figures 3C-D). Similarly, to validate the role of TLR4 signaling in mediating the effects of HPF, we performed studies using ECs pretreated with TLR4 siRNA. Knockdown of TLR4 expression was confirmed with real-time PCR by showing decreased TLR4 expression in the cells treated with TLR4 siRNA, compared to those treated with scrambled siRNA (data not shown). As shown in Figures 3C-D, we found that siRNA knockdown of TLR4 reduced the mRNA levels of some pro-inflammatory molecules (ICAM-1 and E-selectin) under HPF, but not VCAM-1 or MCP-1. This is an interesting finding, because the different results from different TLR4 inhibition approaches, pharmacological inhibitor (CLI-095) which blocks the signaling mediated by the intracellular domain of TLR4 and a more effective inhibitor with siRNA gene silencing, may suggest possible TLR4 mechanisms for future studies. Because TLR4 has more complicated role and relatively minor effects on HPF-mediated responses compared to TLR2, we have focused on illuminating TLR2-mediated signaling underlying endothelial mechanotransduction of flow pulsatility.

Activation of NF-κB in PAECs is induced by HPF and attenuated by TLR2 inhibition or siRNA knockdown

To examine signaling downstream of TLR2 activation caused by HPF, we studied nuclear translocation or activation of NF-κB. As shown in Figure 4A, inhibition of TLR2 with OxPAPC or siTLR2 treatment decreased intranuclear translocation of NF-κB in the cells stimulated with HPF. Also, as the IkappaB kinase complex (IKK) contains two kinase subunits, IKKalpha (IKKα) and IKKbeta (IKKβ), necessary for IkappaB phosphorylation and NF-κB activation, we also examined flow and drug effects on PAEC expression of IKKα and IKKβ. As shown in Figure 4B, HPF enhanced IKKα and IKKβ gene expression and knockdown of TLR2 attenuated this effect. To further examine the role of NF-κB in the inflammatory response of cells to HPF stimulation, the NF-κB inhibitor BAY11-7082 was used. BAY 11–7082 treatment of PAECs led to a reduction in MCP-1 protein expression in response to HPF (Figure 4C).

Circulating media from cells exposed to HPF upregulate the inflammatory responses in normal PAECs through the TLR2/NF-κB pathway

To determine whether TLR2-mediated PAEC inflammation in response to HPF is mediated, at least in part, through endothelial release of damage-associated molecules, we investigated whether there were endogenous signals released from ECs exposed to HPF, which could activate TLR2 triggering an inflammatory response in the absence of flow. We collected the conditioned circulating media from cell cultures under the HPF and LPF conditions (labeled as HPF-FM and LPF-FM, respectively), and then exposed normal bovine PAECs to the conditioned media for 24 h under static conditions. As shown in Figure 5A, cells exposed to HPF-FM produced markedly higher mRNA levels of ICAM-1, VCAM-1, E-selectin and MCP-1 than cells exposed to LPF-FM. Inhibition of TLR2 with OxPAPC or siTLR2 treatment decreased endothelial

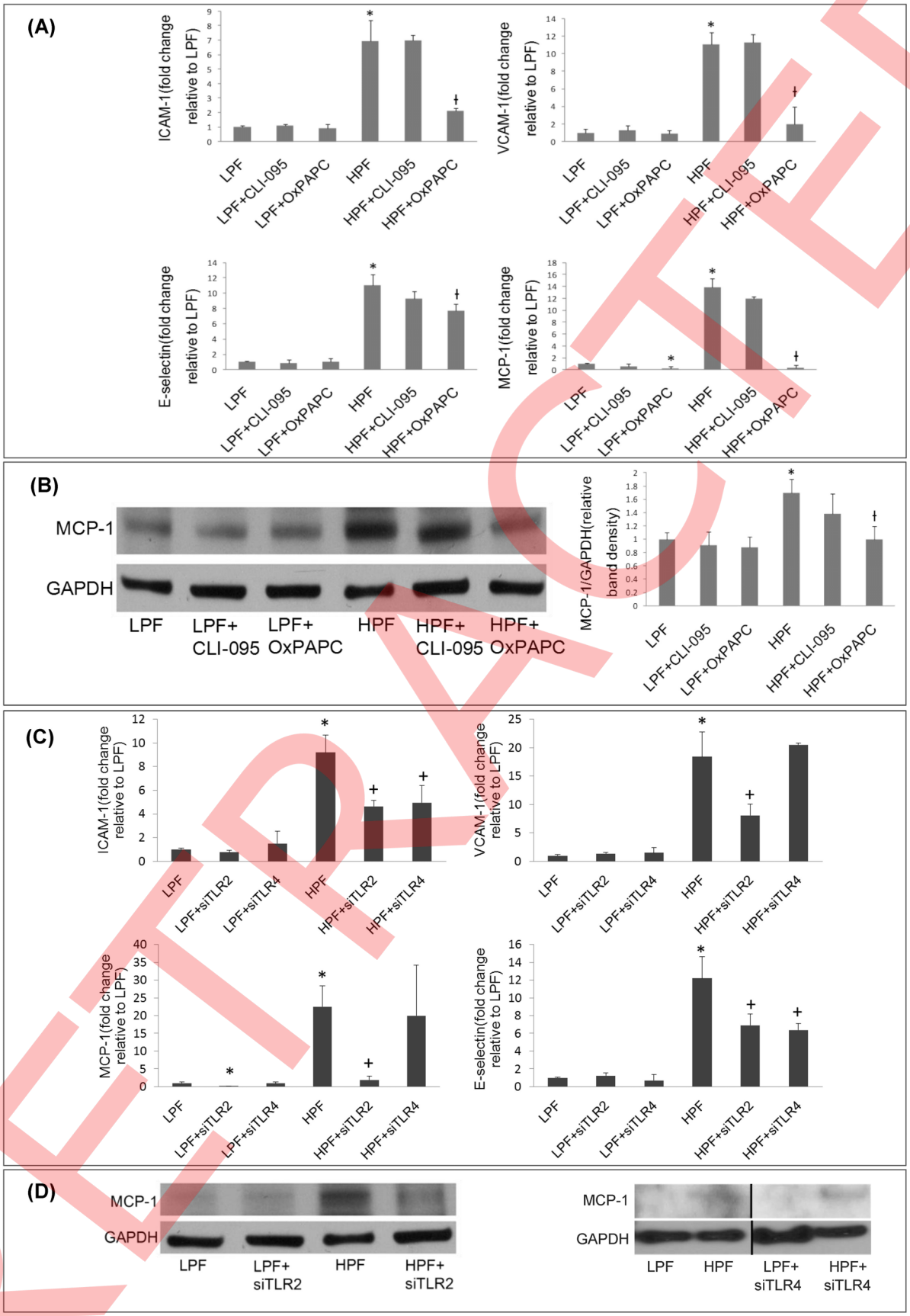
(A)
ICAM-1(fold change relative to LPF)
VCAM-1(fold change relative to LPF)
E-selectin(fold change relative to LPF)
MCP-1(fold change relative to LPF)
LPF
LPF+CLI-095
LPF+OxPAPC
HPF
HPF+CLI-095
HPF+OxPAPC
(B)
MCP-1
GAPDH
LPF
LPF+ CLI-095
LPF+ OxPAPC
HPF
HPF+ CLI-095
HPF+ OxPAPC
MCP-1/GAPDH(relative band density)
(C)
ICAM-1(fold change relative to LPF)
VCAM-1(fold change relative to LPF)
MCP-1(fold change relative to LPF)
E-selectin(fold change relative to LPF)
LPF
LPF+siTLR2
LPF+siTLR4
HPF
HPF+siTLR2
HPF+siTLR4
(D)
MCP-1
GAPDH
LPF
LPF+ siTLR2
HPF
HPF+ siTLR2
LPF
HPF
LPF+ siTLR4
HPF+ siTLR4

Figure 3. Pharmacological or siRNA inhibition of TLR2 results in suppression of PAEC proinflammatory responses caused by stiffening-induced HPF. (A, C) At the mRNA level, TLR2/4 inhibitor OxPAPC or TLR2 siRNA but not TLR4 inhibitor CLI-095, decreased PAEC expression of ICAM-1, VCAM-1, MCP-1 and E-selectin mRNAs under HPF; TLR4 siRNA decreased ICAM-1 and E-selectin but not VCAM-1 and MCP-1 mRNAs. "*": $p<0.05$ versus LPF, "†": $p<0.05$ versus HPF. (B, D) At the protein level, the MCP-1 expression in PAECs exposed to HPF was inhibited by OxPAPC or TLR2 siRNA treatment but not CLI-095 or TLR4 siRNA. The black line in the blot images (D, right) shows separated lanes obtained on the same gel.
doi:10.1371/journal.pone.0102195.g003

expression of ICAM-1, VCAM-1, E-selectin and MCP-1 mRNAs in response to HPF-FM conditioned media. OxPAPC and siTLR2 also decreased HPF-FM induced increases in MCP-1 protein in ECs (Figure 5B). As shown in Figure 5C, inhibition of TLR2 with OxPAPC or siTLR2 treatment also decreased intranuclear translocation of NF-κB in the cells stimulated with HPF-FM.

TLR2 and TLR4 are upregulated in hypertensive pulmonary arterial endothelium

To verify the results obtained in our ex-vivo model system and to confirm that the expression of TLRs and MCP-1 in pulmonary arterial endothelial changes with hypoxia-induced pulmonary hypertension characterized by proximal vascular stiffening [17], we analyzed protein levels in fresh cell lysates of PAECs derived from normal and hypertensive calves using western blotting. Figures 6A and 6B show that distal PAECs from pulmonary hypertensive calves (PH-ECs) exhibited higher levels of MCP-1, TLR2 and TLR4 than control ECs. We also observed that TLR2 expression was upregulated *in vivo* in the endothelium of human patients with IPAH (Figure 6C); as we could not locate bovine TLR antibodies that specifically worked for immunofluorescence.

Discussion

Using a new *in vitro* system, a model illustrating the proximal-distal vascular coupling, we have examined the effects of upstream stiffening on biological changes in downstream endothelium. Herein, silicone tubes with varied moduli and compliances were used to mimic the flow buffering function of proximal pulmonary arteries and resultant hemodynamic effects on changes in downstream arterial endothelium. Using the flow model as well as the hypoxia-induced pulmonary hypertension neonatal calf model characterized by proximal arterial stiffening [17], we have shown that stiffening-induced HPF caused pro-inflammatory responses and upregulated expression of TLRs (TLR2 and TLR4) in "downstream" ECs. We further demonstrated a causal relationship between HPF, TLR2/NF-kB expression and proinflammatory responses in PAECs. The results show that reduced upstream artery compliance induced pro-inflammatory signaling through TLR2. It was also found that TLR2 was upregulated in the freshly separated hypertensive PAECs. Using pharmacologic and siRNA approaches, a role for TLR2 in mediating proinflammatory responses in PAECs in response to HPF was confirmed. To identify the nuclear transcription factor mediating TLR2 flow sensing and pro-inflammatory gene expression, we evaluated the activation of NF-κB in response to low or high flow pulsatility in the presence or absence of a TLR2 inhibitor or gene knockdown and found that TLR2/NF-κB pathway mediated PAEC pro-inflammatory responses. In addition, the finding that conditioned flow media from HPF-stimulated PAEC enhanced TLR2 expression in the normal endothelium suggest that cells under HPF could generate autocrine/paracrine signaling through release of damage-associated molecular patterns (DAMPs) and thus perpetuate endothelial dysfunction through TLR2. Collectively, our findings support the idea that large vascular stiffening could initiate and/or perpetuate inflammatory responses in "downstream" vessels through the TLR2/NF-κB pathway.

Increasing evidence shows that artery stiffening or reduced arterial compliance is a prominent feature of systemic hypertension, pulmonary hypertension and other vascular-related diseases. Only recently have researchers started to relate the coupling of arterial stiffening and consequent flow changes to vascular cell dysfunction [3,5]. However, the mechanisms underlying such coupling remain elusive. Our study illustrates a new potential mechanism in that defective buffering function of a stiffened vessel causes downstream endothelial inflammation by activating TLR2/NF-?B signaling. Using bioengineering principles and polymer technology, we have developed a new flow circulatory system, which reproduces physiological functions of both normal and stiff large arteries in the pulmonary (and perhaps systemic), circulation, provides a physiological link between proximal artery stiffening and hemodynamic environments for distal vascular cells. The mimetic circulatory model, in parallel with animal models, allows investigation of the effects of artery stiffening and flow pulsatility on distal PA remodeling. In pulmonary hypertension, though pulmonary arterial stiffening is increasingly believed to significantly increase right ventricular afterload [6], few have explored its influence on the progression of pulmonary vascular disease which is characterized by progressive endothelial dysfunction and remodeling of downstream small arteries [25]. We previously showed the proinflammatory effects of flow pulsatility on PAECs using a compliance-adjustment chamber [12]. The present study provides more direct *in vitro* and *in vivo* evidence regarding stiffening-induced proinflammatory responses in PAECs, by designing mechanical equivalents of pulmonary arteries to modulate pulse flow waves from a simulated cardiac output, in addition to mechanical and histological characterizations of native human pulmonary arteries. The mechanical properties of blood vessels are designed such that the wall compliance and flow pulsatility are well coupled to maintain vascular homeostasis. Previous studies showed that high distensibility of proximal arteries protects ECs under HPF, but the same flow stimulus has an adverse effect in less compliant vessels such as distal arteries [26].

Consistent with recent studies highlighting on the novel roles of TLR2/4 signaling in cardiovascular diseases such as atherosclerosis and hypertension via endogenous signals from damaged or stressed cells [16,27–30], known as DAMPs, the present study is the first to show that TLR2 was highly upregulated in the small PA endothelium of both calf and human subjects with pulmonary hypertension and stiffened proximal PAs. The mechanistic studies here demonstrate that the underlying mechanism involved in stiffening-induced HPF effects on PAECs is at least partly through flow-induced cell damage that leads to release of TLR ligands. It is possible that these DAMPs could participate in the right heart dysfunction observed in pulmonary hypertension. This proximal-distal coupling mechanism is consistent with the observations of Voelkel et al. that elevated pulmonary vascular pressure alone, without perturbed lung vasculature or involved mediators, do not cause right ventricular failure [31]. These molecules might also contribute to dysfunction of other organs such as kidney and liver, which is also one of characteristics of late stage pulmonary

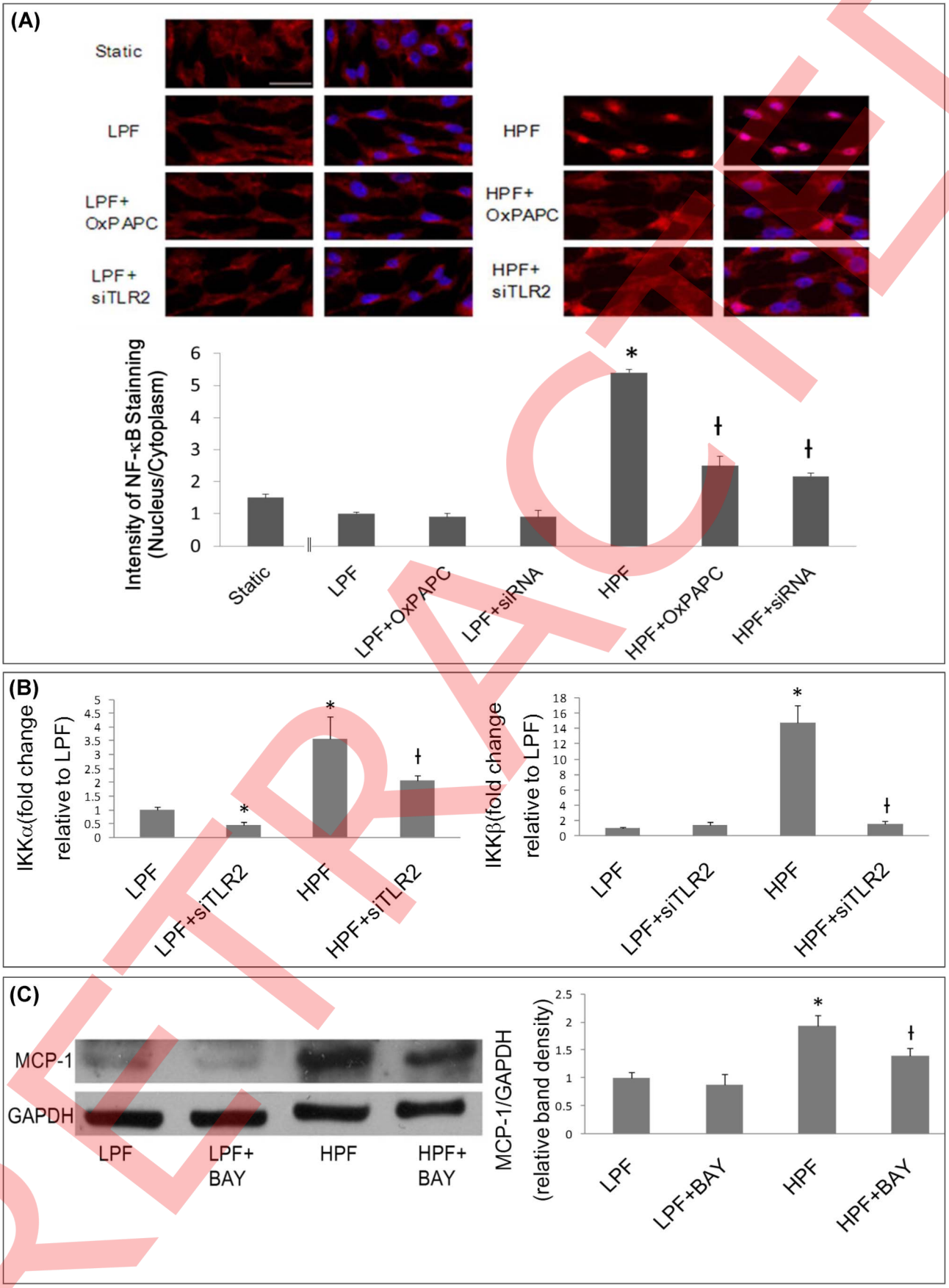
(A)
Static
LPF
LPF+ OxPAPC
LPF+ siTLR2
HPF
HPF+ OxPAPC
HPF+ siTLR2
Intensity of NF-κB Stainning (Nucleus/Cytoplasm)
Static
LPF
LPF+OxPAPC
LPF+siRNA
HPF
HPF+OxPAPC
HPF+siRNA
(B)
IKKα(fold change relative to LPF)
LPF
LPF+siTLR2
HPF
HPF+siTLR2
IKKβ(fold change relative to LPF)
LPF
LPF+siTLR2
HPF
HPF+siTLR2
(C)
MCP-1
GAPDH
LPF
LPF+ BAY
HPF
HPF+ BAY
MCP-1/GAPDH (relative band density)
LPF
LPF+BAY
HPF
HPF+BAY

Figure 4. Activation of TLR2/NF-κB pathway mediated pro-inflammatory responses of PAECs exposed to stiffening-induced HPF. Pulse flow modulates TLR2-induced NF-κB activation in BPAECs. (A) Representative fluorescent images and quantitative measures of NF-kBp65 staining (red) in PAECs show HPF stimulation of PAECs led to increased intranuclear translocation or activation of NF-κB, which was reduced by TLR2/4 inhibitor OxPAPC and TLR2 siRNA. Blue stains show the nuclei. The scale bar shows 50 μm. (B) HPF stimulation of PAECs increased the mRNA levels of IKKα and IKKβ, both of which were attenuated in siRNA-transfected cells with knockdown of TLR2. (C) NF-κB inhibitor (BAY 11–7082) decreased the MCP-1 expression by PAECs exposed to HPF. *: $p<0.05$ versus LPF, †: $p<0.05$ versus HPF.
doi:10.1371/journal.pone.0102195.g004

hypertension. We further established the role of TLR2 in HPF induced endothelial inflammation. Inhibition of TLR2 using pharmacologic (OxPAPC) and molecular (siRNA – siTLR2) approaches reduced NF-kB activation and endothelial inflammation in response to HPF. Though we did not identify specific DAMP ligands induced by HPF, our results using conditioned circulating media to culture normal PAECs demonstrated that molecules released by PAECs stressed under HPF activated PAEC inflammation through TLR2/NF-κB, which could be a mechanism for the endothelium to initiate autocrine signaling. The possible content of the endogenous ligands secreted by PAECs under flow might include heat shock proteins (or HSPs), because HSPs were known as endogenous ligands for TLR2 [32,33] and could be upregulated by pulsatile flow. Damage or stress-induced endogenous TLR2 ligands likely provide continuous support to PAEC dysfunction via autocrine signaling through endogenous TLR2 ligands. In addition to mechanical stimulation with flow, we also used TLR ligands of TLR-2 (peptidoglycan, 10 μg/mL) and TLR-4 (lipopolysaccharide, 200 ng/mL), which similarly upregulated pro-inflammatory stimulation of TLR-2 and TLR-4 pathways (data not shown). Taken together, our findings here, together with new insights into the TLR regulation of inflammation or tissue-damaging responses, provide strong evidence to support evaluation of TLRs as potential targets for the development of new therapies in chronic vascular inflammatory disease where large vessel stiffening is observed. TLR2 and TLR4 are the only TLRs ubiquitously expressed in normal human arteries [34]. Because TLR2 in the endothelium can be upregulated by disturbed flow in atherogenic regions [35] [14], by HPF in distal pulmonary arteries as shown in this study, and by saturated fatty acids [36], targeting TLR2 may be an exciting prospect for the treatment of certain cardiovascular diseases [37,38], especially those characterized by large vessel stiffening.

Compared to TLR2, the role of TLR4 in HPF-mediated proinflammatory responses appears more complicated. Knockdown of TLR4 with specific siRNA, but not TLR4 pharmacological inhibitor CLI-095, decreased part of HPF-induced proinflammatory gene expression. The discrepancy in PAEC responses of different TLR4 inhibitors might be caused by different inhibition mechanisms. CLI-095, also known as TAK-242, is a cyclohexene derivative that suppresses TLR4 signaling mediated by the intracellular domain of TLR4, whereas siRNA gene silencing effectively down-regulates overall TLR4 protein expression, which thus reduces TLR4 signaling through both intracellular and extracellular domains. TLR4 signaling might contribute to the flow-induced inflammation predominantly via extracellular domain. As ECs normally express TLR4 and a very low level of TLR2 [14], absence of TLR4 might also influence EC physiology. Additionally, the discrepancy between TLR4 expression under HPF in the experimental set-up and human situation further suggested the complicated roles of TLR4 in flow-mediated mechanotransduction. TLR4-mediated mechanotransduction of HPF requires further exploration. Recent studies suggested a close relationship between TLR4 and pulmonary hypertension [39].

The present study highlights an important role of TLR2 in regulation of HPF-induced inflammatory response in PAECs. It also shows upregulated expression of TLR4 in hypertensive PAECs; TLR4 reduction inhibited some proinflammatory genes. This is consistent with studies that found greater TLR expression in clinical phenotypes of human pulmonary hypertension [40], and is also consistent with recent literatures showing relevance of TLR to cardiovascular diseases. But it remains unclear from this study why the level of TLR4 is higher in hypertensive PAECs and how it contributes to pathogenesis. In addition, the exact mechanisms underlying DAMP-mediated endothelial inflammation through TLR/NF-κB pathway requires further investigation.

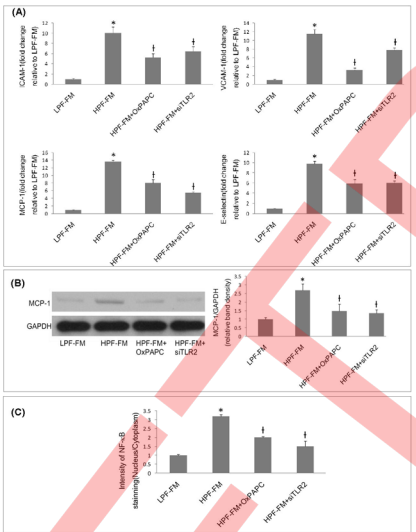

Figure 5. The circulating media from the cells exposed to HPF upregulate the inflammatory responses in normal PAECs through the TLR2/NF-κB pathway. The conditioned circulating media collected from cell cultures under the HPF and LPF conditions, respectively labeled as LPF-FM and HPF-FM, were used to culture normal PAECs for 24 h. (A) The mRNA expressions of ICAM-1, VCAM-1, MCP-1 and E-selectin were upregulated by HPF-FM condition, which were then reduced by OxPAPC and siTLR2. (B) Similar changes were shown in the MCP-1 protein expression. (C) NF-κB intranuclear translocation increased in PAECs stimulated with HPF-FM, which was reduced by OxPAPC and siTLR2. *: $p<0.05$ versus LPF-FM, †: $p<0.05$ versus HPF-FM.
doi:10.1371/journal.pone.0102195.g005

Conclusions

To our knowledge, this is the first report to evaluate the effects of flow pulsatility on TLR signaling in the endothelium and the first to unravel molecular events underlying endothelial mechanotransduction of flow pulsatility. The TLR2/NF-κB pathway in PAECs likely mediates downstream inflammatory responses induced by reduced compliance of upstream vessels which are less capable of dampening HPF, and thus TLR2 might be a potential target for endothelial inflammation of pulmonary hypertension.

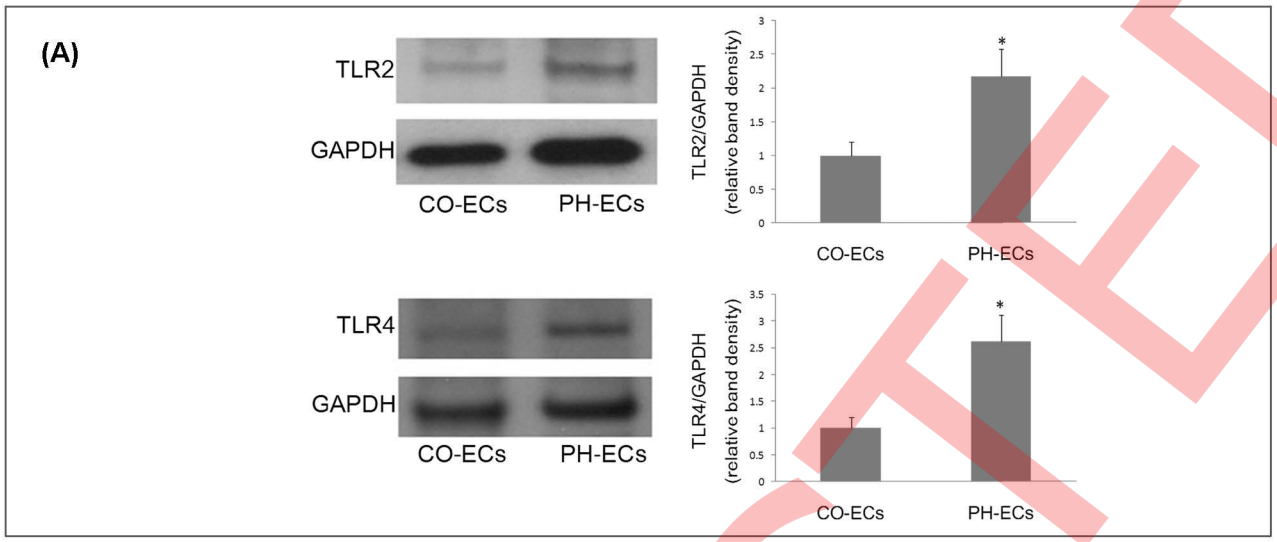
(A)
TLR2
GAPDH
CO-ECs
PH-ECs
TLR2/GAPDH (relative band density)
TLR4
GAPDH
CO-ECs
PH-ECs
TLR4/GAPDH (relative band density)

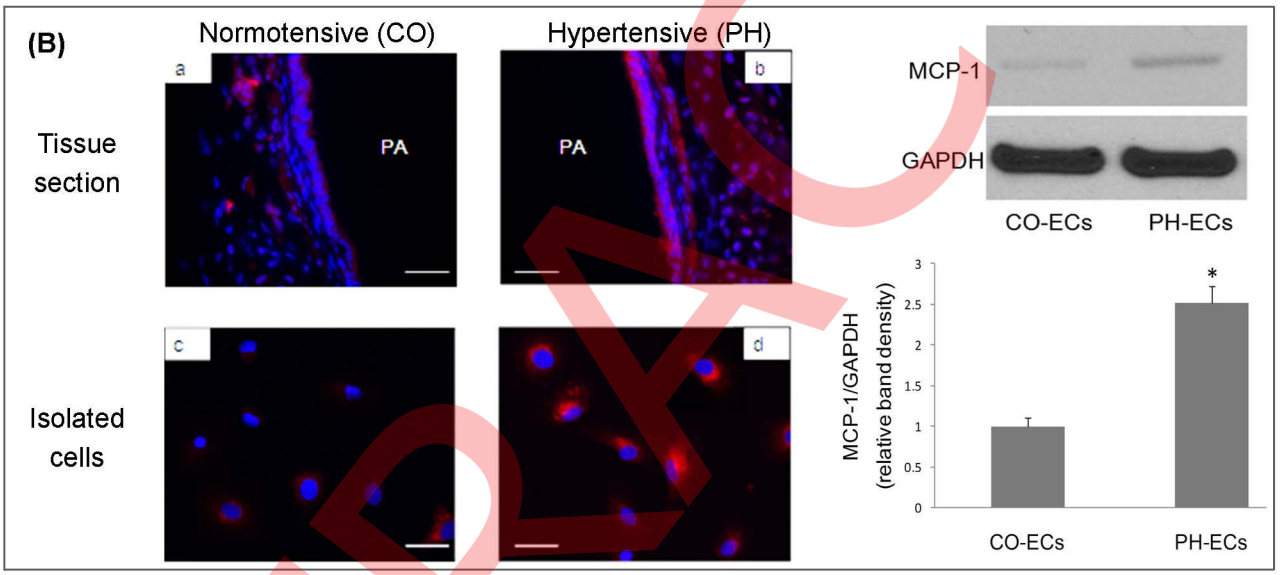
(B)
Normotensive (CO)
Hypertensive (PH)
Tissue section
Isolated cells
a
b
c
d
PA
PA
MCP-1
GAPDH
CO-ECs
PH-ECs
MCP-1/GAPDH (relative band density)
CO-ECs
PH-ECs

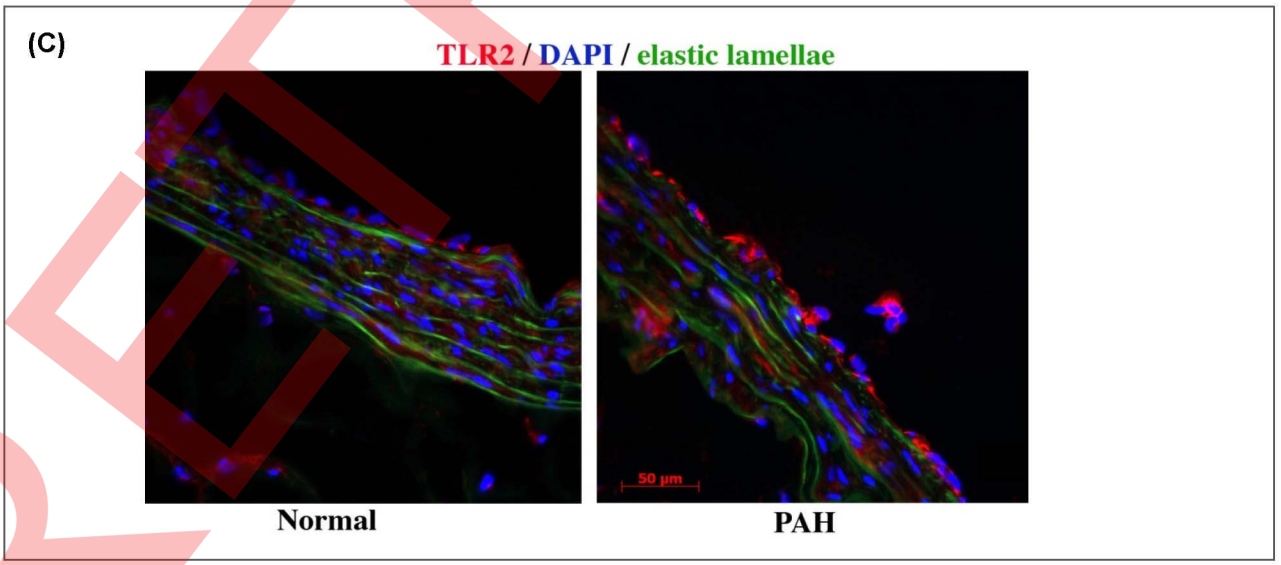
(C)
TLR2 / DAPI / elastic lamellae
50 μm
Normal
PAH

Figure 6. Enhanced TLR and MCP-1 expression in the distal pulmonary artery endothelium *in vivo*. (A) PAECs from calves with hypoxia-induced pulmonary hypertension (PH) show elevated expression of TLR2 and TLR4, compared to control (CO). *:$p<0.05$. (B) Both immunostaining and western blotting results show elevated MCP-1 expression by PH-ECs compared to CO-ECs from calves. "PA" indicates the lumen of a pulmonary artery. *:$p<0.05$. (C) Enhanced TLR2 expression in the pulmonary arterial endothelium of human with pulmonary arterial hypertension (PAH). Cryosections of human intra-lobar pulmonary arteries were immunostained with TLR2 (red fluorescence) and counterstained with DAPI (cell nuclei, blue). Elastic lamellae showed green auto-fluorescence.
doi:10.1371/journal.pone.0102195.g006

Supporting Information

Movie S1 The video illustrating the deformation of a "soft" tube under the normal physiological pulsatile flow condition.
(MOV)

Movie S2 The video illustrating the deformation of a "stiff" tube under the normal physiological pulsatile flow condition.
(MOV)

Acknowledgments

The authors would like to thank Dr. Maria Frid for her help with tissue samples, Dr. Xianzhong Meng for his advice on TLR signaling and for providing human TLR antibodies and Qingchun Zeng for his help with experiments. Lung tissues from idiopathic PAH patients and control subjects were kindly provided by Dr. Barbara Meyrick and obtained from the Pulmonary Hypertension Breakthrough Initiative (PHBI), which is funded by the Cardiovascular Medical Research Education Fund (CMREF). The tissues were procured at the Transplant Procurement Centers at Stanford University, University of California, San Diego, Vanderbilt University and Allegheny General Hospital.

Author Contributions

Conceived and designed the experiments: YT DW HZ KS JH WT. Performed the experiments: YT HZ PT. Analyzed the data: KH WT. Contributed reagents/materials/analysis tools: WT. Wrote the paper: YT WT KS.

References

1. Adji A, O'Rourke MF, Namasivayam M (2011) Arterial stiffness, its assessment, prognostic value, and implications for treatment. Am J Hypertens 24: 5–17.
2. Hashimoto J, Ito S (2011) Central pulse pressure and aortic stiffness determine renal hemodynamics: pathophysiological implication for microalbuminuria in hypertension. Hypertension 58: 839–846.
3. Mitchell GF, van Buchem MA, Sigurdsson S, Gotal JD, Jonsdottir MK, et al. (2011) Arterial stiffness, pressure and flow pulsatility and brain structure and function: the Age, Gene/Environment Susceptibility—Reykjavik study. Brain 134: 3398–3407.
4. Lammers S, Scott DE, Hunter K, Tan W, Shandas R, et al. (2012) Mechanics and function of the pulmonary vasculature: Implications for pulmonary vascular disease and right ventricular function. Compr Physiol 1: 1–25.
5. Zachariah JP, Xanthakis V, Larson MG, Vita JA, Sullivan LM, et al. (2012) Circulating vascular growth factors and central hemodynamic load in the community. Hypertension 59: 773–779.
6. Wang Z, Chesler NC (2011) Pulmonary vascular wall stiffness: An important contributor to the increased right ventricular afterload with pulmonary hypertension. Pulm Circ 1: 212–223.
7. Burton A, editor (1966) Physiology and biophysics of the circulation. Chicago: Year Book.
8. Chiu RCJ (1995) Biophysics of pulsatile perfusion. J Thorac Cardiovas Surg 109: 810.
9. Chiu JJ, Chien S (2011) Effects of disturbed flow on vascular endothelium: pathophysiological basis and clinical perspectives. Physiological reviews 91: 327–387.
10. Davies PF (2009) Hemodynamic shear stress and the endothelium in cardiovascular pathophysiology. Nature clinical practice Cardiovascular medicine 6: 16–26.
11. Hahn C, Schwartz MA (2009) Mechanotransduction in vascular physiology and atherogenesis. Nature reviews Molecular cell biology 10: 53–62.
12. Li M, Scott DE, Shandas R, Stenmark KR, Tan W (2009) High pulsatility flow induces adhesion molecule and cytokine mRNA expression in distal pulmonary artery endothelial cells. Ann Biomed Eng 37: 1082–1092.
13. Curtiss LK, Tobias PS (2009) Emerging role of Toll-like receptors in atherosclerosis. J Lipid Res 50 Suppl: S340–345.
14. Dunzendorfer S, Lee HK, Tobias PS (2004) Flow-dependent regulation of endothelial Toll-like receptor 2 expression through inhibition of SP1 activity. Circ Res 95: 684–691.
15. Li X, Jiang S, Tapping RI (2010) Toll-like receptor signaling in cell proliferation and survival. Cytokine 49: 1–9.
16. Erridge C (2009) The roles of Toll-like receptors in atherosclerosis. J Innate Immun 1: 340–349.
17. Tian L, Lammers SR, Kao PH, Reusser M, Stenmark KR, et al. (2011) Linked opening angle and histological and mechanical aspects of the proximal pulmonary arteries of healthy and pulmonary hypertensive rats and calves. Am J Physiol Heart Circ Physiol 301: H1810–1818.
18. Lau EM, Iyer N, Ilsar R, Bailey BP, Adams MR, et al. (2012) Abnormal pulmonary artery stiffness in pulmonary arterial hypertension: in vivo study with intravascular ultrasound. PLoS One 7: e33331.
19. Sanz J, Kariisa M, Dellegrottaglie S, Prat-Gonzalez S, Garcia MJ, et al. (2009) Evaluation of pulmonary artery stiffness in pulmonary hypertension with cardiac magnetic resonance. JACC Cardiovasc Imaging 2: 286–295.
20. Hunter KS, Albietz JA, Lee PF, Lanning CJ, Lammers SR, et al. (2010) In vivo measurement of proximal pulmonary artery elastic modulus in the neonatal calf model of pulmonary hypertension: development and ex vivo validation. J Appl Physiol 108: 968–975.
21. Grignola JC, Domingo E, Aguilar R, Vazquez M, Lopez-Messeguer M, et al. (2011) Acute absolute vasodilatation is associated with a lower vascular wall stiffness in pulmonary arterial hypertension. Int J Cardiol.
22. Paz R, Mohiaddin RH, Longmore DB (1993) Magnetic resonance assessment of the pulmonary arterial trunk anatomy, flow, pulsatility and distensibility. Eur Heart J 14: 1524–1530.
23. Reuben SR (1971) Compliance of the human pulmonary arterial system in disease. Circ Res 29: 40–50.
24. Li M, Scott DE, Shandas R, Stenmark KR, Tan W (2009) High pulsatility flow induces adhesion molecule and cytokine mRNA expression in distal pulmonary artery endothelial cells. Ann Biomed Eng 37: 1082–1092.
25. Stenmark KR, McMurtry IF (2005) Vascular remodeling versus vasoconstriction in chronic hypoxic pulmonary hypertension: a time for reappraisal? Circ Res 97: 95–98.
26. Peng X, Haldar S, Deshpande S, Irani K, Kass DA (2003) Wall stiffness suppresses Akt/eNOS and cytoprotection in pulse-perfused endothelium. Hypertension 41: 378–381.
27. McCarthy CG, Goulopoulou S, Wenceslau CF, Spitler K, Matsumoto T, et al. (2014) Toll-like receptors and damage-associated molecular patterns: novel links between inflammation and hypertension. American journal of physiology Heart and circulatory physiology 306: H184–196.
28. Mian MO, Paradis P, Schiffrin EL (2014) Innate immunity in hypertension. Current hypertension reports 16: 413.
29. Singh MV, Chapleau MW, Harwani SC, Abboud FM (2014) The immune system and hypertension. Immunologic research.
30. Spirig R, Tsui J, Shaw S (2012) The Emerging Role of TLR and Innate Immunity in Cardiovascular Disease. Cardiology research and practice 2012: 181394.
31. Bogaard HJ, Natarajan R, Henderson SC, Long CS, Kraskauskas D, et al. (2009) Chronic pulmonary artery pressure elevation is insufficient to explain right heart failure. Circulation 120: 1951–1960.
32. Erridge C (2010) Endogenous ligands of TLR2 and TLR4: agonists or assistants? Journal of leukocyte biology 87: 989–999.
33. Hochleitner BW, Hochleitner EO, Obrist P, Eberl T, Amberger A, et al. (2000) Fluid shear stress induces heat shock protein 60 expression in endothelial cells in vitro and in vivo. Arteriosclerosis, thrombosis, and vascular biology 20: 617–623.
34. Pryshchep O, Ma-Krupa W, Younge BR, Goronzy JJ, Weyand CM (2008) Vessel-specific Toll-like receptor profiles in human medium and large arteries. Circulation 118: 1276–1284.
35. Mullick AE, Soldau K, Kiosses WB, Bell TA 3rd, Tobias PS, et al. (2008) Increased endothelial expression of Toll-like receptor 2 at sites of disturbed blood flow exacerbates early atherogenic events. J Exp Med 205: 373–383.
36. Jang HJ, Kim HS, Hwang DH, Quon MJ, Kim JA (2013) Toll-like receptor 2 mediates high-fat diet-induced impairment of vasodilator actions of insulin.

American journal of physiology Endocrinology and metabolism 304: E1077–1088.
37. Bertocchi C, Traunwieser M, Dorler J, Hasslacher J, Joannidis M, et al. (2011) Atorvastatin inhibits functional expression of proatherogenic TLR2 in arterial endothelial cells. Cellular physiology and biochemistry : international journal of experimental cellular physiology, biochemistry, and pharmacology 28: 625–630.
38. Higashikuni Y, Tanaka K, Kato M, Nureki O, Hirata Y, et al. (2013) Toll-like receptor-2 mediates adaptive cardiac hypertrophy in response to pressure overload through interleukin-1beta upregulation via nuclear factor kappaB activation. Journal of the American Heart Association 2: e000267.
39. Bauer EM, Chanthaphavong RS, Sodhi CP, Hackam DJ, Billiar TR, et al. (2014) Genetic deletion of toll-like receptor 4 on platelets attenuates experimental pulmonary hypertension. Circulation research 114: 1596–1600.
40. Broen JC, Bossini-Castillo L, van Bon L, Vonk MC, Knaapen H, et al. (2011) A rare polymorphism in the gene for Toll-like receptor 2 is associated with systemic sclerosis phenotype and increases the production of inflammatory mediators. Arthritis Rheum 64: 264–271.